Technical University of Denmark

System security assessment in real-time using synchrophasor measurements

Jóhannsson, Hjörtur; Wache, Markus

Published in:
Proceedings of 2013 IEEE PES Innovative Smart Grid Technologies

DOI:
10.1109/ISGTEurope.2013.6695484

Publication date:
2013

Document Version
Early version, also known as pre-print

Link to publication

Citation (APA):
Jóhannsson, H., & Wache, M. (2013). System security assessment in real-time using synchrophasor measurements. In Proceedings of 2013 IEEE PES Innovative Smart Grid Technologies . IEEE. DOI: 10.1109/ISGTEurope.2013.6695484

System Security Assessment in Real-Time using synchrophasor measurements

Hjörtur Jóhannsson
Center for Electric Power and Energy,
Department of Electrical Engineering,
Technical University of Denmark
Kgs. Lyngby, Denmark

Markus Wache
Siemens AG,
Infrastructure & Cities Sector,
Smart Grid Division
Nurnberg, Germany

***Abstract* —The increasing amount of renewable power from wind and solar generation causes higher fluctuation in power generation and in general increased distances between generation and load. Both aspects influence the system stability of electricity transmission in a negative way. Therefore, additional measures to ensure stable and secure operation of the system are necessary. Time stamped synchrophasor measurements lay the foundation for development of new real-time applications for security and stability assessment. The paper provides overview of existing solutions for synchrophasor based security assessment and sheds light on ongoing research activities that focus on exploiting wide-area synchrophasor measurements for real-time security assessment of sustainable power systems. At last, an mathematical mapping enabling informative visualization of the system state in respect to aperiodic rotor angle stability is described and analyzed in detailed.**

***Index Terms*—Synchrophasor, PMU, Wide Area Monitoring, System Security, Control Room Application, Visualization**

I. INTRODUCTION

Stable and secure power systems are of fundamental importance to modern societies and will continue to be so in the future. The global challenges to electric power systems in the coming decades are great where focus is on energy supply with a minimal dependency on fossil fuels which requires that a large share of electric power production needs to be based on sustainable energy sources.

A power production that is a subject to prevailing weather conditions can introduce rapid changes in the system operating conditions, resulting in that planning for stable and secure operation can no longer be made few hours ahead. The fluctuating power production introduces a need for short-horizon supervision and fast planning and coordination of control actions that ensure system security in real-time.

The development of Phasor Measurement Units (PMUs) [1], based on extremely accurate GPS-satellite time-stamping, opened up the possibility for obtaining synchronized wide-area "snapshots" of the system conditions as frequently as once per cycle of system frequency. This makes it possible to obtain, in real time, a data set that provides full observability of the system conditions and that can be used for assessment of the operating conditions. In the future, wide-area measurement-based technologies are expected to be increasingly incorporated into the protection and control of the system [2-5].

This paper sheds light on ongoing research activities that focus on exploiting wide-area synchrophasor measurements for real-time security assessment of sustainable power systems. Overview of a recent method for real-time assessment is presented and focus is on presenting the details of a mathematical mapping that enables informative visualization of multiple operating points in respect to aperiodic rotor angle stability.

II. WIDE AREA MONITORING WITH SYNCHROPHASORS

Wide area monitoring based on distributed, fast and time-stamped phasor measurements, acquired by PMUs, offers significant benefits compared to measurements from Remote Terminal Units (RTU) as described in table 1.

TABLE 1: SIGNIFICANT DIFFERENCES BETWEEN RTU AND PMU

Measurements via RTU	Synchrophasors from PMU
Updated slowly (typical every 5 s)	Fast update with reporting rate up to once per cycle of system frequency
No time correlation for measurements	Every measurement has a timestamp
RMS values without phase angles	Phasor values with amplitude and phase angle for voltage and current

The high repetition rate of the PMU measurements enables real time monitoring of the dynamic motion of power systems. Power swings, frequency response, loss of network element and other phenomena in transmission and distribution network may be observed in high details and with a little delay.

The improved visibility of dynamic phenomena is becoming more and more important due to increased penetration of non-controllable renewable energy sources

The authors would like to acknowledge the Danish Council for Strategic Research for their support of this work.

(RES) into power systems. With increasing share of power production based on RES causes less predictability in the power flow patterns in the grid and causes increased fluctuations in the system operating point.

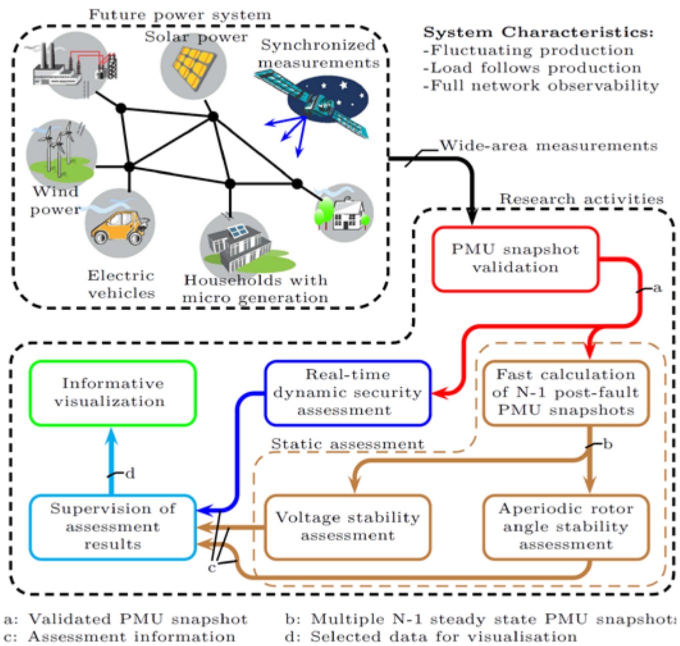

Figure 1: *Overview of research activities in the SOSPO project related to real-time security assessment based on synchronphasor measurements.*

III. Overview of The SOSPO Project

The Danish research project, "Secure Operation of Sustainable Power Systems" (SOSPO) launched early 2012 and focusses among others on the development of an integrated operational tool for system operators that supports secure operation of the future sustainable power system. Special attention is paid to the development of methods for real-time stability and security assessment.

The project focusses on solutions for a future power system with the following characteristics:

- A very high share of the power production capability is based on fluctuating sustainable energy sources.
- The power system states are observed in real time by PMU measurements.

Fig. 1 provides an overview over the different research activities related to real-time security assessment in the SOSPO project. The overall functionality of the security assessment tools developed in the project is represented by six individual modules as illustrated in Fig. 1. Synchronized PMU measurements are received in real time by the validation module which ensures consistency of the measured data. The validated PMU snapshots are used as input for methods for performing dynamic security assessment and a set of methods performing static security assessment. The research activities related to the static assessment involve the development of methods for fast determination of the N-1 post-fault PMU snapshots. The N-1 snapshots are used as input to real-time stability assessment methods, where in the project the focus is put on the assessment of long-term voltage stability and further development of a method for assessing aperiodic small-signal rotor-angel stability [6-8].

The output from the security assessment modules serves as an input to the supervision module where the assessment information is collected and analysed in order to obtain coherent picture of the security of the system. The supervision module sends information to the visualization module to visualize the current operating conditions for system operators and assist in taking appropriate control actions to ensure system integrity.

IV. Application Example of Wide Area Monitoring

In [8] a new method for real-time assessment of electric power systems was presented. The approach used is to carry out an element-wise assessment of a particular mechanism of stability. The stability condition that this method focusses on is whether equilibrium between the steady state mechanical torque and the counteracting electrical torque, within each machine in the system, can be maintained.

In order to assess the conditions of a given generator, only two system quantities are needed; the system Thevenin impedance seen from the generator's node of power injection and the corresponding injection impedance measured from the same node. It is essential that the generator's node of power injection is represented at a node were the generator's steady state voltage is constant. In [7] expression is derived for the boundary of maximum power that a given generator can inject into a node of constant voltage magnitude. The Thevenin impedance determines the boundary, which can be expressed in terms of injection impedance by:

$$\mathrm{Z_{inj}} = \frac{Z_{th}\sin\theta}{\cos\varphi_{th}} \tag{1}$$

Where $\overline{Z_{inj}} = Z_{inj} < \theta$ is the complex injection impedance and $\overline{Z_{th}} = Z_{th} < \varphi_{th}$ is the complex Thevenin impedance. The above equation represents a circle in the injection impedance plane that intersects the origin of the plane, and the points where $\overline{Z_{inj}} = -\overline{Z_{th}}$ and $\overline{Z_{inj}} = \overline{Z_{th}^*}$. The stability of a given generator is determined by inspecting whether the measured value of the injection impedance is inside or outside this circle. A value of the injection impedance outside the boundary represents stable operation while a value inside the circle represent unstable operation, characterized by that a small increase in the steady state voltage phase angle at the node of injection would result in reduction in the generator's injected power. With the injection and Thevenin impedances known, the following assessment criteria can be expressed [8]:

$$\left|\frac{\overline{Z_{inj}}\,2\sin\varphi_{th} + j\cdot Z_{th}}{Z_{th}}\right| \begin{cases} > 1, & \text{stable} \\ < 1, & \text{unstable} \\ = 1, & \text{on boundary} \end{cases} \tag{2}$$

The presented assessment criterion is based on analytically derived expression for the generators' stability boundary, which forms the basis for very fast assessment. The most time critical part of the method is to determine the Thevenin impedance of the individual generators. In [9], results from a test of a new algorithm computing the information needed for carrying out aperiodic rotor angle stability show that the stability conditions of 1325 generators in a 7917 bus system can be determined in approximately 2 ms, thereby forming the base for real-time assessment of large systems in the millisecond range. The results in [9], are expected to support an effective adaption of existing offline methods for dynamic security assessment to real-time operation [10]. The short assessment times enables fast assessment of the system security where N-1 post fault snapshots could be used to quickly determine whether a given contingency would cause aperiodic rotor angle instability.

The presented assessment critera in (2) indicates only whether the given generator is stable or unstable. For the purpose of providing decision support, it would be useful if the generator's margin to its stability boundary could be expressed in terms of system quantities that are meaningful and intuitive to a system operator. In [8], it is shown that a percentage active power margin, expressed in terms of the generator's Thevenin and injection impedance can be expressed as:

$$\%\Delta P = \frac{\cos(\delta + \varphi_{th}) + 1}{1 + \left|\frac{\overline{Z_{inj}}}{\overline{Z_{th}+Z_{inj}}}\right| cos\varphi_{th}} \cdot 100\% \qquad (3)$$

The above margin describes how much the generator's active power injection can be increased as the generator's voltage phase angle δ at the node of injection is increased to its critical value while other system variables are fixed. The margin obtained reflects therefore only changes in one system variable, the voltage phase angle δ. This is different from how stability margins are derived by means of continuation methods where the system is stressed in a particular direction by applying some predefined loading and dispatch patterns. The selection of such stress patterns is usually based on the operational experience, where the daily consumption patterns are usually well known by the system operators.

Even though the above suggested stability margins, derived from the phase angle margin Δδ, are not obtained by applying specific "normal" stress patterns they do anyhow provide useful information. The method is intended to provide a stability assessment during emergency operating conditions. During such conditions, it is not likely that the normal stress patterns would give the most likely stress direction of the system, since many other control and load restoration mechanisms have a more significant role in such situations. The actual stress direction might be dominated by the actions of ULTC-transformers and other devices that try to restore the pre-disturbance consumption. This means that the "normal" stress direction is not suitable for determining a margin to the system stability boundary. On the other hand, the presented element-wise margins provide valuable information concerning which of the generators is operating close to, or approaching its stability or security boundaries.

V. INFORMATIVE VISUALIZATION OF OPERATING POINTS

In [7], analytical expressions were derived, in terms of injection impedance, for curves of constant voltage magnitude, phase angle, active and reactive power. The curves provide meaningful information regarding how the conditions of a given generator may be interpreted when knowing only the value of the injection and Thevenin impedance. Figure 2 provides an overview of how the curves of constant P, Q, δ and V appear in the injection impedance plane.

The radius of the circle representing the stability boundary expressed by (1) is dependent both the magnitude and angle of $\overline{Z_{th}}$. In fact, all of the curves of constant values of P,Q,V and δ depend on the modulus and the argument of $\overline{Z_{th}}$. In a system having K generators, K different stability boundaries exists, where each boundary is held against one injection impedance value. For the purpose of enabling informative visualization of multiple operating points, it is desirable that a mapping of a given operating point $\{\overline{Z_{inj}}, \overline{Z_{th}}\}$ is provided such that all of the K different operating points are held against the same stability boundary and that some of the meaningful information presented in figure 2 is preserved after the mapping.

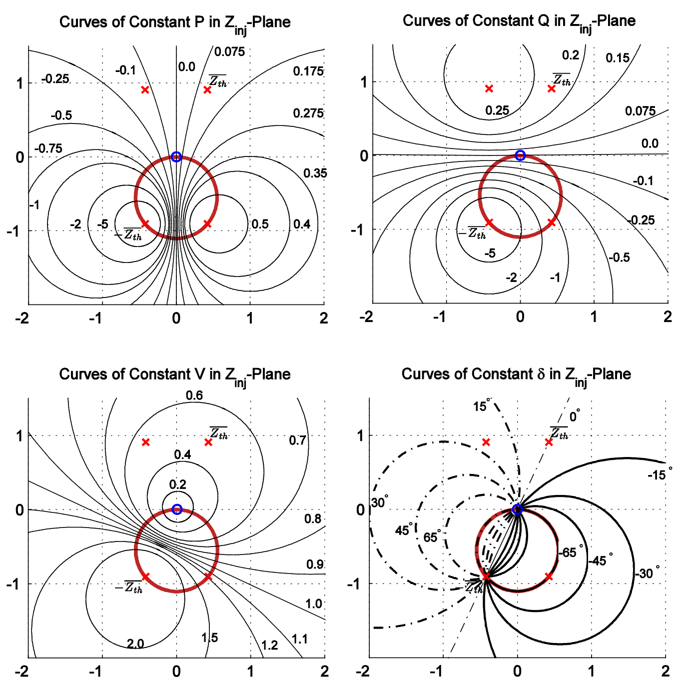

Figure 2: *Characteristic curves of constant P, Q, V and Delta in injection impedance plane. The values of P and Q are normalized by* $\boldsymbol{S_{base}} = \boldsymbol{E_{th}^2}/\boldsymbol{Z_{th}}$ *and* $\boldsymbol{E_{th}}$ *is a base value for V.*

An arbitrary operating point $\{\overline{Z_{inj,0}}, \overline{Z_{th,0}}\}$ can be mapped into another impedance plane as the point $\{\overline{Z_{inj,*}}, Z_{th,0} < 90°\}$, where the information regarding the phase angle margin to the boundary $\Delta\delta$ and the voltage ratio V/E_{th} is preserved after the mapping. Such mapping is given by [8]:

$$\overline{Z_{inj,*}} = \frac{1}{Y_{inj,0} + Y_{th,0}(1 - e^{j(90° - \varphi_{th})})} \qquad (4)$$

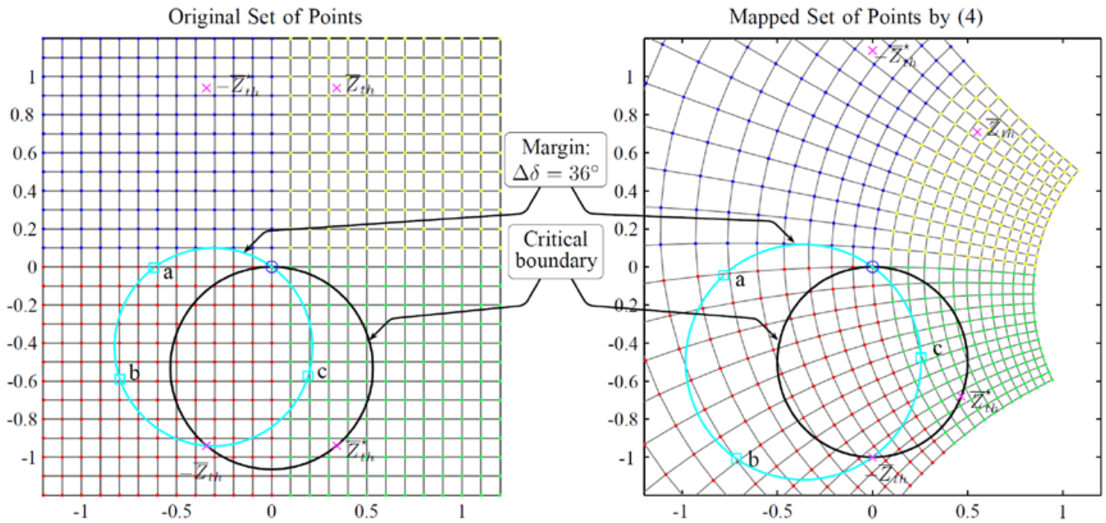

Figure 3: Illustration of the mapping of injection impedances when (4) is applied. To the left, the critical boundary (in black) and the circle representing the conditions where $\Delta\delta$ is 36° (in light blue), when $\overline{Z_{th}} = 1 < 70°$. To the right, mapping of all points in the left into a impedance plane where $\overline{Z_{th,*}} = 1 < 90°$.

Figure 3 illustrates the effect of the mapping of injection impedances according to (4). The plot to the left shows an equally meshed grid in the injection impedance plane, the stability boundary when $\overline{Z_{th}} = 1 < 70°$ (the black circle) and a line of constant $\Delta\delta$ that is 36° away from the boundaries (light blue circle). To the right, the results when (4) is applied. Each of the mapped injection impedance points is such that the voltage magnitude and the phase angle difference to the critical boundary have been preserved. The stability boundary appears now as a circle with diameter at unity, which is the same as the boundary obtained when $\overline{Z_{th}} = 1 < 90°$ and the blue line represents the line of constant phase angle when $\delta = 54°$, which corresponds to a phase angle margin $\Delta\delta = 36°$. Figure 3 illustrates that an arbitrary operating point $\{\overline{Z_{inj,0}}, \overline{Z_{th,0}}\}$ can be mapped as the point $\{\overline{Z_{inj,*}}, Z_{th,0} < 90°\}$, by utilizing (4) where characteristics concerning $\Delta\delta$ and the voltage ratio V/E_{th} are preserved after the mapping. In order to visualize multiple operating points in the same impedance plane, further manipulation of (4) is needed so that the same normalized stability boundary can be applied to all of the K operating points for the K system generators.

By manipulating the expression in (4), the stability boundaries can normalized in such a way that they appear as a unit circle centered at the origin of the normalized impedance plane:

$$\overline{Z_{inj,*,pu}} = \frac{2 \cdot \overline{Z_{inj,*}}}{Z_{th,0}} + j \qquad (5)$$

Using the above expression, the characteristic curves for constant $\Delta\delta$, V/E_{th} and the stability boundary can be used to visualize all of the K operating points $\{\overline{Z_{inj,i}}, \overline{Z_{th,i}}\}$ in the same impedance plane, where the same boundary applies to all operating points. This means that an arbitrary operating point can be visualized in the normalized impedance plane shown in fig. 5, by applying the mapping described in (5)

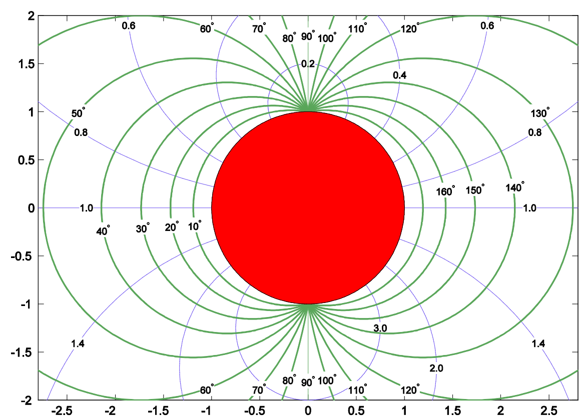

Figure 5: The normalized impedance plane in which an arbitrary operating point can be depicted by using (5).

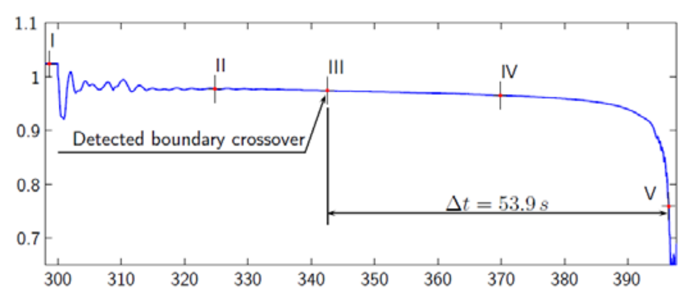

Figure 6: Bus voltage in simulated blackout scenario used to demonstrate the informative visualization in figure 7.

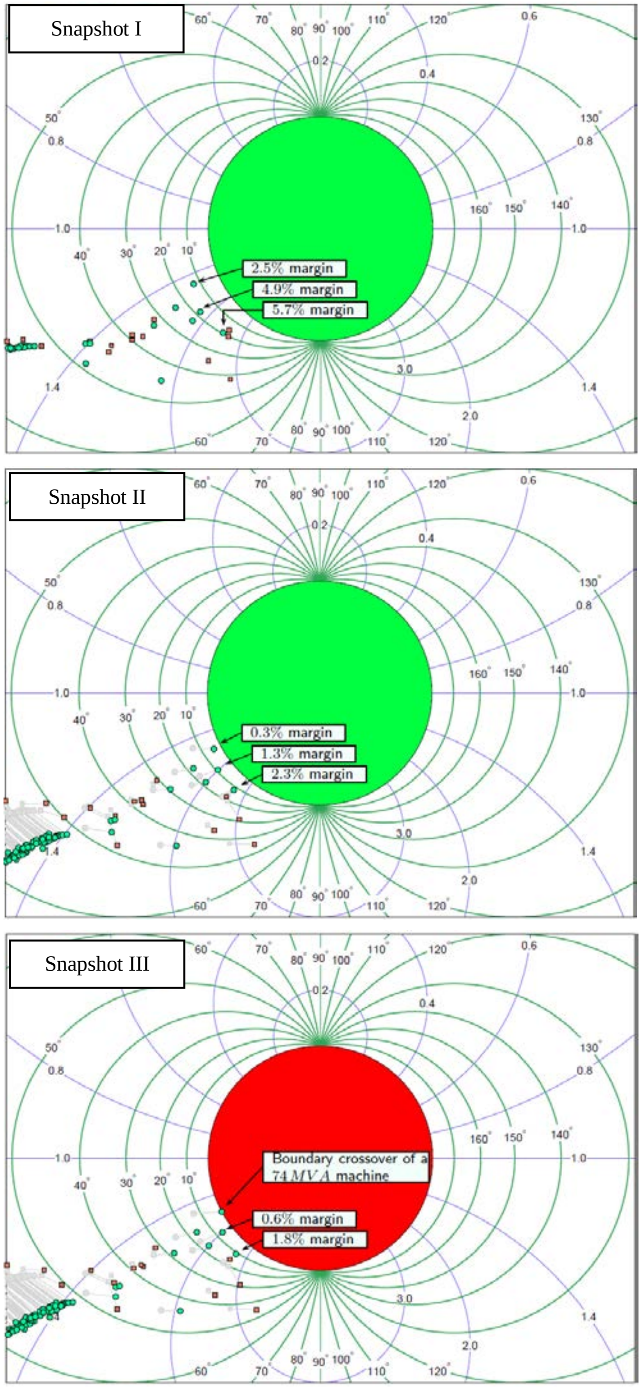

Figure 7: Snapshots I-III as marked in figure 6. The most critical generators are easily identified early on, thereby providing the operator information about the exact location and the nature of the emerging problem.

1) Example of an informative visualization:

In [8], an instability simulation of a 488 bus, 144 generator system is presented. Figure 6 shows the results of a time domain simulation of a selected bus voltage, where the occurrence of aperiodic rotor angle stability is characterized by the rapid collapse in voltage magnitude.

Figure 7 shows the system conditions at selected snapshots from the time domain simulation. Snapshot I shows the pre fault conditions where all machines have significant active power margin to the boundary. The visualization enables quick identification of the critical machines in the system immediately after the major disturbance (snapshot II). In snapshot III, the first machine crosses the boundary which eventually causes collapse in voltage 55 seconds later (snapshot IV in figure 6). Such visualization provides a system operator useful means for decision support, since the operator can easily identify which are the critical machines, monitor their distance-to-instability and the nature of the emerging problem. All of these factors provide the basis for finding effective countermeasures that would to avoid the machines to cross the stability boundary.

VI. Conclusion

The paper discussed the benefits of using PMUs for security assessment of future sustainable power systems and shed a light on-going research activities that focus on exploiting wide-area measurements for real-time security assessment. An overview of a resent real-time assessment method was presented where a focus was on elaborating on the informative visualisation of multiple operating points. The characteristics of a mathematical mapping were presented and explored in details, where it was illustrated how the visual information concerning curves of constant voltage magnitude and phase angle margin are preserved after the mapping of any given operating point for a generator. The mapping of the generators' operating points enables informative visualisation of the system conditions in respect to a particular mechanism of instability. The provided example demonstrated how the condition of all system generators could be depicted in the same picture, providing means for obtaining a quick visual overview of the system conditions and identification of potentially critical machines.

References

[1] A. Phadke, J. Thorp, M. Adamiak; 'A New Measurement Technique for Tracking Voltage Phasors, Local System Frequency, and Rate of Change of Frequency', IEEE Trans. Power App. Syst 102(5), 1025–1038.,1983.

[2] M. Begovic, D. et al.; "Wide-Area Protection and Emergency Control," Proc. IEEE, vol. 93, no. 5, pp. 876–891, May 2005.

[3] A. G. Phadke, et al.; "The Wide World of Wide-Area Measurement". IEEE Power Energy Mag., vol. 6, no. 5, pp. 52-65. Sep-Oct 2008.

[4] C. Taylor, et al.; "WACS-Wide-Area Stability and Voltage Control System: R&D and Online Demonstration," Proc. IEEE, May 2005.

[5] O. Samuelsson, M. Hemmingsson, A. H. Nielsen, K. O. H. Pedersen, J. Rasmussen; "Monitoring of power system events at transmission and distribution level", IEEE Trans. on Power Syst., vol: 21, issue: 2, 2006.

[6] H. Jóhannsson, et al. "Real-time stability assessment based on synchrophasors," in PowerTech, 2011 IEEE Trondheim, Jun. 2011

[7] H. Jóhannsson, et al. "Identification of critical transmission limits in injection impedance plane," INT J ELEC POWER, vol. 43, no. 1, 2012.

[8] H. Jóhannsson, "Development of early warning methods for electric power systems," PhD dissert., Technical University of Denmark, 2011.

[9] S. Sommer and H. Jóhannsson, "Real-time thevenin impedance computation," in IEEE PES ISGT Wahsington, Washington, 2013.

[10] T. Weckesser, et al, "Investigation of the adaptability of transient stability assessment methods to real-time operation," in IEEE PES ISGT Europe, Berlin, 2012.